Measurements of Low-Energy Protons Using a Silicon Detector for Application to SEE Testing

C Cazzaniga, RG Alia, A Coronetti, K Bilko, Y Morilla, P Martin-Holgado, M Kastriotou, CD Frost

Published version information

Citation: C Cazzaniga et al. Measurements of Low-Energy Protons using a Silicon Detector for Application to SEE Testing. IEEE Trans Nucl Sci 69, no. 3 (2021): 485-490
DOI: 10.1109/TNS.2021.3123814

Measurements of Low-Energy Protons using a Silicon Detector for Application to SEE Testing

Carlo Cazzaniga, Rubén García Alía, Andrea Coronetti, Kacper Bilko, Yolanda Morilla, Pedro Martin-Holgado, Maria Kastriotou and Christopher D. Frost

***Abstract*— A silicon detector with a fast electronics chain is used for the dosimetry of protons in the range 0.5-5 MeV at the CNA 3 MV Tandem laboratory in Seville, Spain. In this configuration, measurements can be performed in pulsed mode, using a digitizer to record event-by-event proton energy depositions. The distributions of deposited energy were obtained thanks to a calibration with an alpha source. Measurements of flux and deposited energy are used to enable SEE testing on selected SRAMs.**

***Index Terms*— Low-energy protons, silicon detector, single event effects.**

I. Introduction

Single Event Effects (SEEs) are one of the major concerns for the reliability of electronics in space. Prediction and mitigation methodologies have been developed by industry, based on characterizations with high-energy protons and heavy ions, and are defined in standards [1].

However, in the past decade, several studies have shown that the contribution of the direct ionization from low energy protons has a potentially significant impact on the accuracy of prediction methods used to calculate the upset rate [2-6]. The issue became more acute with the miniaturization of electronics in deep sub-micron technologies [7-10]. Through direct ionization, low energy protons (E < 3 MeV) can deposit in the device sensitive volume an amount of energy exceeding the critical charge. This mechanism is strongly enhanced for those protons with energy near the Bragg peak. That is, those protons that deposit their energy entirely in the sensitive volume.

According to recent studies for space applications, low-energy proton single-event effects are a large contribution to the error rate for technologies at and below the 45 nm node [11], and effects cannot be well-quantified, that is their cross-sections cannot be easily estimated, using alphas or other ions as a proxy [12]. This is particularly relevant for proton-rich environments, e.g., High-altitude LEO trajectories or trajectories crossing Earth's Van Allen Belts [13, 14]. It is also worth mentioning the importance for systems exposed to unshielded solar particle events, when low energy proton fluxes can be strongly enhanced [15, 16].

Low energy proton testing of electronic devices is a novelty that has only recently started to appear in space standards [1]. Although protons of these energies can be extracted from many Van de Graaf or Cyclotrons, there are only a limited number of facilities characterized for this application, and beamlines are not specifically designed for SEE testing, needing upgrade in terms of infrastructure and dosimetry instrumentation. For this reason, we have performed experimental work to equip a multipurpose beamline at the tandem facility of the *Centro Nacional de Aceleradores* (CNA) in Spain for this application [17].

In this context, we propose a detector based on a silicon diode to be used for the dosimetry of low energy protons. Silicon detectors are widely used in high-energy physics and nuclear physics experiments [18] and recent developments have been pushed by the application of digital acquisition systems [19, 20]. The detector, with some differences in the electronic chain, was used successfully for dosimetry of high energy neutrons and mixed field [21, 22], and ultra-high energy ions [23-25]. Here we present measurements performed with protons of energies in the range of 0.5-5 MeV. The detector allows for extending the measurable flux range of the facility to $10^2 – 10^{12}$ $cm^{-2}s^{-1}$.

These dosimetry measurements allowed for a study on proton direct ionization for SRAMs used in space applications [26]. In the present work, a selected case serves as an example to discuss the requirements for the dosimetry system.

Manuscript received on July 16, 2021. Carlo Cazzaniga, Maria Kastriotou and Christopher D. Frost are with ISIS Facility, UKRI-STFC, Rutherford Appleton Laboratory, Didcot OX11 0QX, UK. (e-mail: carlo.cazzaniga@stfc.ac.uk). Rubén García Alía and Kacper Bilko are with CERN, CH-1211, Genève, Switzerland. Yolanda Morilla and Pedro Martin-Holgado are with Centro Nacional de Aceleradores (Universidad de Sevilla, CSIC, JA). , 41092-Sevilla, Spain. Andrea Coronetti is with CERN and Department of Physics, University of Jyväskylä, 40014 Jyväskylä, Finland.

II. Experimental Setup

2.1 Description of the facility

The test campaign was performed at the CNA 3 MV Tandem laboratory, using protons of energies ranging from 500 keV to 5.9 MeV [27, 28].

To perform experiments with low energy protons the devices under test (DUT) need to be placed in vacuum and must be appropriately delidded before the test campaign to allow sufficient penetration to the sensitive volume. The beam is transported in vacuum (~10^{-6} mbar) from the tandem up to the irradiation chamber. Different electrical feedthroughs have been connected in order to bias and monitor "in situ" the response of the devices during the irradiation.

In order to obtain low fluxes (lower than 10^8 $cm^{-2}s^{-1}$) and large uniform irradiation areas (e.g., 18 x 18 cm^2, as in this campaign), a beam *sweeping* technique is needed. This is achieved choosing the corresponding magnetic field intensity for the selected amplitude components in a 2D beam-rastering system. The two magnets of this system operate with 0.05 Hz out-of-phase frequency values in the range of 20-30 Hz. In this way, the beam, which has a pencil area of about 1 cm^2 covers the entire surface in a recursive pattern with a good fluence uniformity (on the order of 90%).

The sample holder assembly, with an aluminum variable slit in front, is electrically insulated from the rest of the line. This assembly is biased at 200-300 V, in order to collect the secondary electrons, and connected to a current integrator with the purpose of monitoring the flux in a Faraday Cup configuration. The lower limit of this instrument for measuring currents is roughly 50 pA, corresponding approximately to fluxes above 10^6 $cm^{-2}s^{-1}$ considering this irradiation area. This lower limit is not defined by the sensitivity of the integrator itself, which could measure currents below 50 pA, but by the residual electromagnetic noise that is still present after the optimization of the setup.

As we present in this work, a Si diode can be used for monitoring the flux in the complementary range 10^2 – 10^6 $cm^{-2}s^{-1}$.

2.2 Description of the detector and electronics

The silicon detector is a fully depleted p-n junction diode manufactured by Micron Semiconductors Ltd. The geometry of the silicon (2 mm x 2 mm x 140 µm) features a square face, a ceramic printed circuit board (PCB) and a metal housing.

In the vacuum chamber, the detector is connected to a low-noise current preamplifier (Cividec C2) with an analog bandwidth of 2 GHz and a gain of 40 dB. From the preamplifier the coaxial connections are fed through to the outside of the vacuum chamber. The reverse bias (+40 V) is given by an ORTEC model 710 bias supply. The signal output is fed to a channel of a CAEN digitizer model DT5751, 1 Gsample/s - 10 bits. This is used in oscilloscope mode: all the waveforms triggering above threshold are recorded, including their time stamps. The waveforms are then analysed offline. A schematic of the experimental setup is presented in Fig. 1.

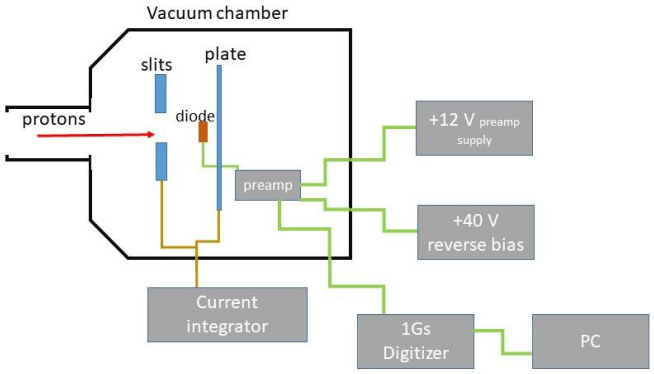

Fig. 1. Schematics of the experimental setup in the vacuum chamber (not to scale).

The picture in Fig. 2 shows the Si diode mounted on the sample holding plate, next to a microelectronics DUT (an SRAM, 65nm, 16 Mbit, by Cypress - now Infineon - Reference CY62167GE30-45ZXI). Only one sample is irradiated in each test. A scintillator, also visible in the picture, is used in preparation of experiments for beam alignment.

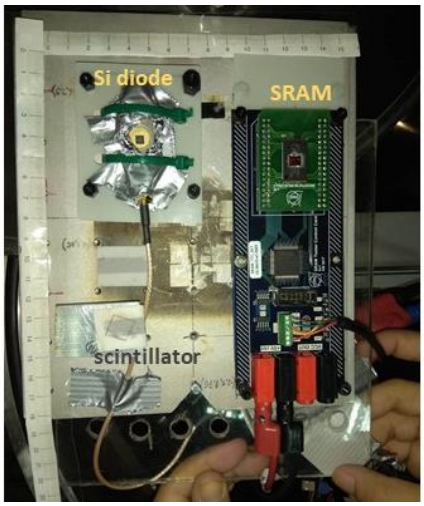

Fig. 2. Picture of the devices under irradiation.

Although out of the scope of this work, it is worth mentioning that, when irradiating 10^{15} protons/cm^2 on silicon detectors, displacement damage effects are

expected. The changes in the silicon bulk will cause an increase of the reverse current as well as a decrease of the charge collection efficiency. Good reviews about displacement damage in silicon and their parametrization can be found in [29, 30].

III. Measurements

3.1 Waveforms

This signal processing chain has been designed to provide fast signals for high counting rate applications, where pile-up can be an issue. In fact, when operating in pulse mode "low currents" of a fraction of nA, i.e., fluxes up to 10^6 p/cm^2/s, can be considered "high fluxes".

Moreover, the fact that the beam is *sweeping* a larger area, as explained above, means that the instantaneous flux during the sweep can be much higher than the average flux.

Examples of measured waveforms induced by proton interaction in the silicon detector are shown in Fig. 3. Here one can see that the signals are very fast, < 10 ns wide (FWHM).

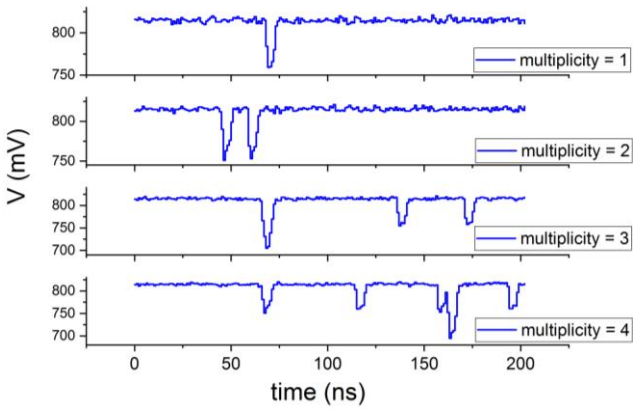

Fig. 3. Examples of proton waveforms as recorded by the 1 Gs digitizer during proton irradiation.

The digital acquisition records a waveform each time a signal is above threshold. We defined these waveforms to be 200 ns wide. This value was chosen to be about 20 times the length of a single pulse, in order to be long enough to capture multiple pulses trailing close together, but short enough not to overload the data buffer of the digitizer. Most of the times, there is a single pulse within this waveform, as in the example with *multiplicity=1*. In some cases, there are multiple proton-induced pulses in the same waveform, as in the other examples (*multiplicity>1*). In these cases the pulses can be easily discriminated off-line during the analysis by a simple algorithm that imposes a software threshold. In some cases pileup is still present: see as an example *multiplicity=4* of Fig. 3, where the third pulse, despite being counted as one, is clearly due to pile-up. However, we find that these events are rare enough to be only a second order effect on the results, unless when the system is operating close to the higher flux limit. Fig. 4 represents probability distributions for three cases with relatively high flux. For example, with a flux of $2\cdot10^4$ cm^{-2}s^{-1}, we observe that 87% of the events have *multiplicity* = 1, 10% have *multiplicity = 2*, and only the remaining 3% have higher multiplicity. As the flux increases, the probability of *multiplicity = 1* becomes smaller (here in the example it becomes 40% for $2\cdot10^5$ cm^{-2}s^{-1}). The probability of a larger multiplicity increases accordingly with increased fluxes.

3.2 Energy Calibration and Resolution

When using a current preamplifier the deposited energy is proportional to the pulse area [21]. A calibration of the detector in its final setup was performed at CNA in vacuum using a triple-alpha source (^{239}Pu, ^{241}Am and ^{244}Cm), which features three alpha lines at the known energies of 5157 keV, 5486 keV and 5805 keV. The calibration spectrum is shown in Fig. 5 with Gaussian fits of the three peaks. The calibration in energy with the triple alpha source is obtained with a linear fit. The energy resolution (≈ 2 % FWHM) is good for such a fast digital electronic chain. A better resolution could be obtained with an analog spectroscopic chain (charge preamplifier and amplifier with μs shaping time), but this setup would not be able to handle high fluxes. In this case, there is a tradeoff between resolution and high counting rate capabilities.

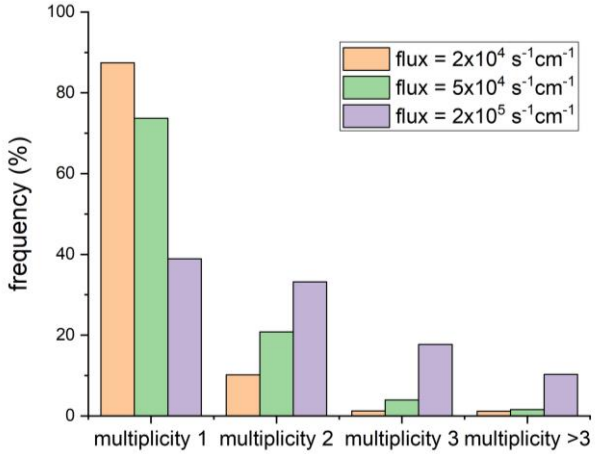

Fig. 4. Frequency of occurrence of event multiplicity. Data is shown for three selected fluxes.

3.3 Measurements of Proton Deposited Energy

Energy spectra of each irradiation run can be built to study the protons' deposited energy.

Fig. 6 shows examples of runs in the whole energy range. Fig. 6a shows spectra in the range 1.5-3 MeV. According to the thickness of the silicon diode, protons with energy < 3 MeV are fully stopped within the silicon. Therefore, the main component of the spectra at these energies is the full energy peak. We can notice the good energy resolution and that there are some structures of lower energies, which could be protons with degraded energy, present in the beam due, for example, to interaction with the collimation slits. Fig. 6b shows spectra in the range 0.5-1 MeV. Here the resolution is slightly compromised, due to the fact that for smaller signal the electronic noise is relatively more relevant.

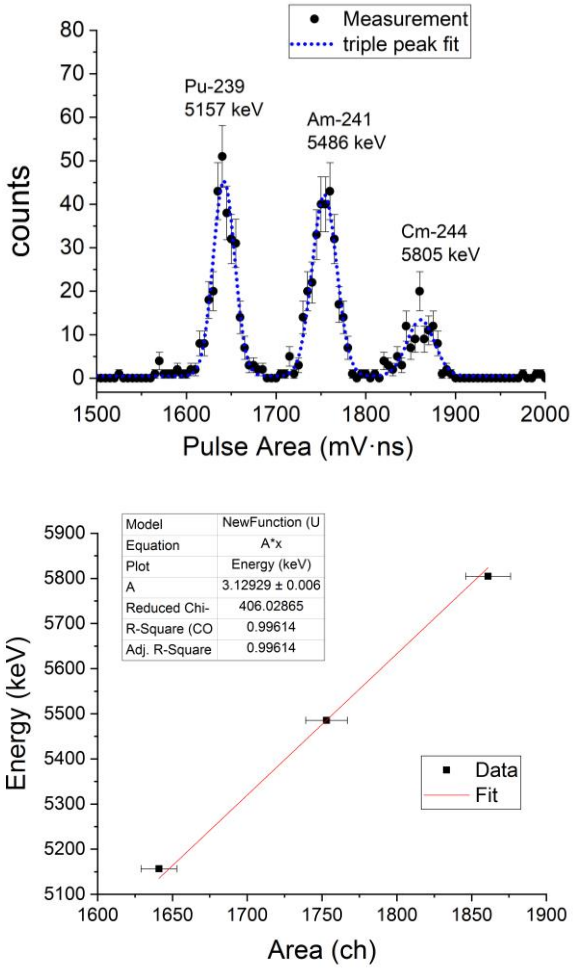

Fig. 5. Pulse area spectrum measured with a calibration triple-alpha source of ^{239}Pu, ^{241}Am and ^{244}Cm (top). Linear calibration of deposited energy as a function of pulse area (bottom).

However, we can still notice that some peaks are definitely broader than others, in particular those with the most reduced flux. We can speculate that this could be associated with the beam transport. Finally, Fig. 6c shows spectra for energies > 3 MeV. We can see that protons at 4 and 5 MeV are *punching through* the detector. The energy of the proton is not fully deposited and the peaks are larger due to straggling. It is interesting to see that for E = 4 MeV some residual of the full energy peak is still present, due to the deflection of protons to wide angles, which allows them to go through a longer path in the silicon and stop.

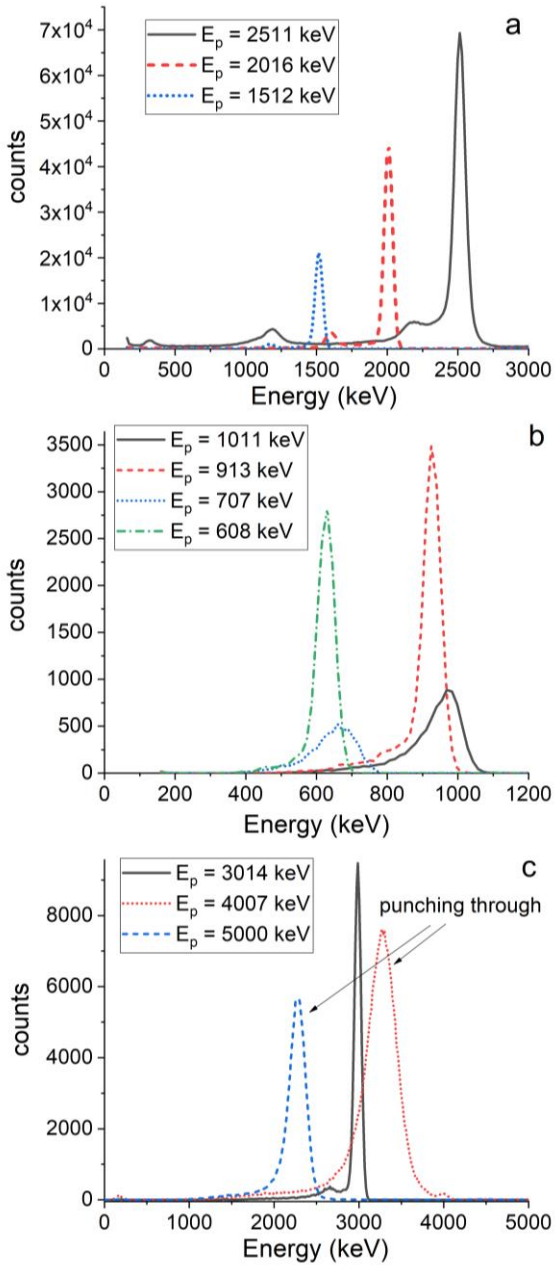

Fig. 6. Energy spectra measured with a silicon diode under low energy proton irradiation at CNA.

Plotting, as in Fig. 7, the average measured proton energy vs. the nominal energy given by the accelerator we can confirm the linearity of the system, which is crucial for dosimetry. Here we included all the measurements where the full energy peak is present.

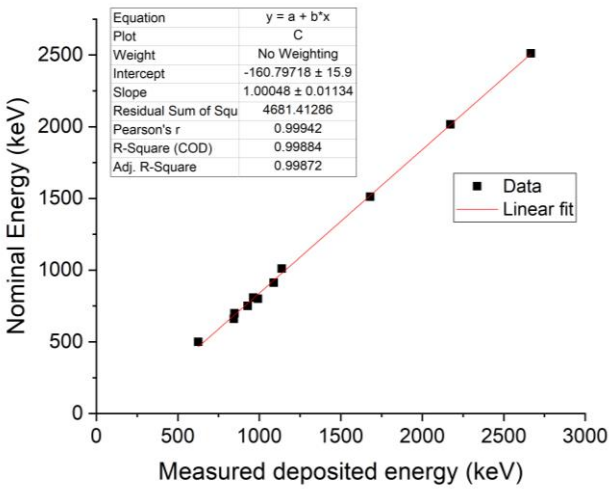

Fig. 7. Measured vs. nominal proton energy. At this scale, considering the achieved energy resolution of about 2% FWHM, error bars are of a size comparable to the square markers.

IV. Dosimetry Results for SEE Testing

During this irradiation campaign, where the silicon diode has been used for dosimetry, three different commercial SRAMs, and a custom development SRAM, were tested. Details and results are presented in [26]. The data for all the SRAMs are in [31].

Here, in Fig. 8, we present, as an example, the results of one of the devices, a 65 nm-16 Mbit SRAM by Cypress, now Infineon, Reference CY62167GE30-45ZXI.

The important thing to notice is that the cross section spans over about 6 orders of magnitude. The peak region cross-section is caused by the fact that, after traversing the back-end-of-line, the protons have a residual kinetic energy of a few keV, i.e., very close to the Bragg peak. Therefore, the energy deposited can exceed, even by far, the critical charge. At higher energy, e.g., above 2 MeV, protons are not as affected and have more limited linear energy transfer. So, upsets by direct ionization are less likely and upsets by other mechanisms, e.g., nuclear elastic and inelastic scattering and electromagnetic Coulomb scattering are more likely [32], though FLUKA is currently not correctly equipped to reproduce SEUs from all these processes (thus the differences between experimental and numerical data above 2 MeV).

The strong cross-section variability is what motivates the use of a wide range of fluxes. Fluxes in the range 10^2 – 10^8 $cm^{-2}s^{-1}$ have been used in these tests. The silicon diode was necessary to extend the flux capabilities in terms of dosimetry to the range 10^2 – 10^6 $cm^{-2}s^{-1}$.

It is relevant to notice the good agreement of FLUKA [33, 34] simulations (see [26] for details) with measurements, in particular in the range 0.5-2 MeV.

As we can see, the upper limit of flux detection with the silicon in pulse mode is very close to the lower limit of detection of the Faraday cup. This is probably why we have a discrepancy of about a factor of 2 on the only point where both systems were operating effectively. However, we also notice that, if discarding this point, we have a smooth transition of the curve measured with the silicon diode and the one measured with the Faraday cup integrator.

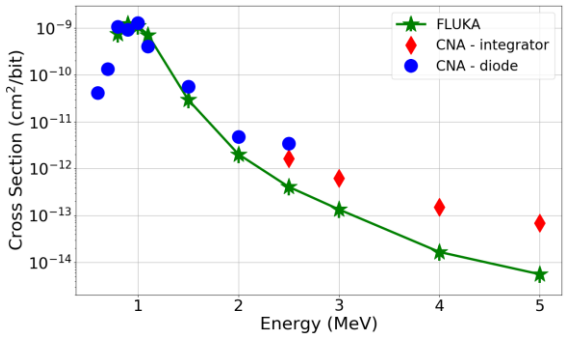

Fig. 8. Measured cross section of an SRAM, where dosimetry was performed either with the silicon diode or with a Faraday cup integrator. Results are compared to Monte Carlo simulations (FLUKA). Error bars, obtained considering counting statistics, are of smaller size than the markers, also due to the logarithmic scale.

V. Conclusions

It has been demonstrated how a silicon detector can be used for dosimetry of low energy protons in the 0.5-5 MeV range. It was shown that a fast electronic chain is needed for operating in pulse mode. The system was calibrated with an alpha source, enabling measurements of the deposited energy of protons. The dosimetry provided by the silicon diode allowed extending the flux range of the facility, resulting in the successful study of SEE cross sections of selected SRAMs.

References

[1] *Single Event Effects Test Method and Guidelines*, Standard ESCC 25100, European Space Components Coordination, ESA, Oct. 2014, [Online]. Available: https://escies.org/ Accessed on: Oct. 20, 2021.

[2] N. A. Dodds *et al*., "Hardness Assurance for Proton Direct Ionization-Induced SEEs Using a High-Energy Proton Beam," *IEEE Trans. Nucl. Sci.*, vol. 61, no. 6, pp. 2904-2914, Dec. 2014, doi: 10.1109/TNS.2014.2364953.

[3] J. Guillermin, N. Sukhaseum, P. Pourrouquet, N. Chatry, F. Bezerra and R. Ecoffet, "Worst-Case Proton Contribution to the Direct Ionization SEU Rate," *in Proc. 2017 RADECS Conf.*, Geneva, Switzerland, Oct. 2017, pp. 330-337, doi: 10.1109/RADECS.2017.8696135.

[4] B. Ye *et al*., "Low energy proton induced single event upset in 65 nm DDR and QDR commercial SRAMs." *Nucl. Instrum. Methods Phys. Res. B*, vol. 406, pp. 443-448, Sept. 2017.

[5] L. D. Edmonds and K. J. Edmonds, "A Method for Estimating SEU Rates From Protons by Direct Ionization," *IEEE Trans. Nucl. Sci.*, vol. 55, no. 5, pp. 2666-2678, Oct. 2008, doi: 10.1109/TNS.2008.2002203.

[6] C. Weulersse, F. Miller, D. Alexandrescu, E. Schaefer and R. Gaillard, "Assessment and comparison of the low energy proton sensitivity in 65nm to 28nm SRAM devices," *in Proc. 2011 RADECS Conf.*, Sevilla, Spain, Sept. 2011, pp. 291-296, doi: 10.1109/RADECS.2011.6131399.

[7] N.A. Dodds *et al.*, "The contribution of low-energy protons to the total on-orbit SEU rate," *IEEE Trans. Nucl. Sci.*, vol. 62, no. 6, pp. 2440-2451, Nov. 2015.

[8] B.D. Sierawski *et al.*, "Impact of low-energy proton induced upsets on test methods and rate predictions," *IEEE Trans. Nucl. Sci.*, vol. 56, no. 6, pp. 3085-3092, December 2009.

[9] K.P. Rodbell, D.F. Heidel, H.H.K. Tang, M.S. Gordon, P. Oldiges, and C.E. Murray, "Low-energy proton-induced single-event-upsets in 65 nm node, silicon-on-insulator, latched and memory cells," *IEEE Trans. Nucl. Sci.*, vol. 54, no. 6, pp. 2474-2479, December 2007.

[10] D.F. Heidel et al., "Low energy proton single-event-upset test results on 65 nm SOI SRAM," *IEEE Trans. Nucl. Sci.*, vol. 55, no. 6, pp. 3394-3400, December 2008.

[11] N. Seifert, B. Gill, J. A. Pellish, P. W. Marshall and K. A. LaBel, "The Susceptibility of 45 and 32 nm Bulk CMOS Latches to Low-Energy Protons," *IEEE Trans. Nucl. Sci.*, vol. 58, no. 6, pp. 2711-2718, Dec. 2011, doi: 10.1109/TNS.2011.2171004.

[12] J. A. Pellish *et al*., "Criticality of Low-Energy Protons in Single-Event Effects Testing of Highly-Scaled Technologies," *IEEE Trans. Nucl. Sci.*, vol. 61, no. 6, pp. 2896-2903, Dec. 2014, doi: 10.1109/TNS.2014.2369171.

[13] G. Hubert, S. Duzellier, F. Bezerra and R. Ecoffet, "MUSCA SEP3 contributions to investigate the direct ionization proton upset in 65nm technology for space, atmospheric and ground applications," *in Proc. 2009 RADECS Conf.*, Bruges, Belgium, Sept. 2009, pp. 179-186, doi: 10.1109/RADECS.2009.5994577.

[14] E. H. Cannon *et al*., "Heavy Ion, High-Energy, and Low-Energy Proton SEE Sensitivity of 90-nm RHBD SRAMs," *IEEE Trans. Nucl. Sci.*, vol. 57, no. 6, pp. 3493-3499, Dec. 2010, doi: 10.1109/TNS.2010.2086482.

[15] Labrador, A. W., et al. "Solar-particle energy spectra during the large events of October-November 2003 and January 2005." in *Proceedings of the 29th International Cosmic Ray Conference.* Vol.1. Tata Institute of Fundamental Research , Pune, India, pp. 111-114, April 2005.

[16] McGuire, R. E., and T. T. Von Rosenvinge. "The energy spectra of solar energetic particles." *Adv. Space Res.*, vol. 4.2-3, pp. 117-125, 1984.

[17] Y. Morilla et al., "Progress of CNA to become the Spanish facility for combined irradiation testing in aerospace", *in Proc. 2018 RADECS Conf.* Gothenburg, Sweden, pp. 250-254, Sep. 2018.

[18] W. Sadrozinski, "Applications of silicon detectors," *IEEE Trans. Nucl. Sci.*, vol. 48, no. 4, pp. 933-940, Aug. 2001, doi: 10.1109/23.958703.

[19] M. Alderighi *et al*., "Charge identification in large area planar silicon detectors, using digital pulse shape acquisition," *IEEE Trans. Nucl. Sci.*, vol. 53, no. 1, pp. 279-285, Feb. 2006, doi: 10.1109/TNS.2006.869827.

[20] A. Vignati, et al. "Innovative thin silicon detectors for monitoring of therapeutic proton beams: preliminary beam tests." *J. Instrum.* Vol. 12, Art. no. C12056, Dec. 2017.

[21] C. Cazzaniga *et al*., "Study of the Deposited Energy Spectra in Silicon by High-Energy Neutron and Mixed Fields," *IEEE Trans. Nucl. Sci.*, vol. 67, no. 1, pp. 175-180, Jan. 2020

[22] C. Cazzaniga *et al*., "Fast neutron measurements with solid state detectors at pulsed spallation sources." *J. Neutron Res.*, vol. 22, no. 2-3, pp. 345-352, Oct. 2020.

[23] V. Wyrwoll *et al*., "Longitudinal Direct Ionization Impact of Heavy Ions on See Testing for Ultrahigh Energies," *IEEE Trans. Nucl. Sci.*, vol. 67, no. 7, pp. 1530-1539, July 2020, doi: 10.1109/TNS.2020.2994370.

[24] C. Cazzaniga et al., "Measurements of ultra-high energy lead ions using silicon and diamond detectors." *Nucl. Instrum. Methods Phys. Res. A*, vol. 985, Art. no. 164671, Jan. 2021.

[25] M. Kastriotou *et al*., "Single Event Effect Testing With Ultrahigh Energy Heavy Ion Beams," *IEEE Trans. Nucl. Sci.*, vol. 67, no. 1, pp. 63-70, Jan. 2020, doi: 10.1109/TNS.2019.2961801.

[26] A. Coronetti *et al.*, "Assessment of proton direct ionization for the radiation hardness assurance of deep sub-micron SRAMs used in space applications", *IEEE Trans. Nucl. Sci*., vol. 68, no. 5, pp. 937-948, May 2021.

[27] J. García López *et al.*, "CNA: The first accelerator-based IBA facility in Spain." *Nucl. Instrum. Methods Phys. Res. B,* vol.161, pp. 1137-1142, Mar. 2000.

[28] M.A. Respaldiza, *et al.*, "Accelerator-based research activities at "Centro Nacional de Aceleradores", Seville (Spain)." *Nucl. Instrum. Methods Phys. Res. B*, vol. 266, pp. 2105-2109, May 2008.

[29] M. Moll, "Displacement Damage in Silicon Detectors for High Energy Physics," *IEEE Trans. Nucl. Sci*., vol. 65, no. 8, pp. 1561-1582, Aug. 2018, doi: 10.1109/TNS.2018.2819506.

[30] G. Lindström, "Radiation damage in silicon detectors." *Nucl. Instrum. Methods Phys. Res. A*, vol. 512.1-2, pp. 30-43, Oct. 2003.

[31] A. Coronetti et al., "SEU characterization of commercial and custom-designed SRAMs based on 90-nm technology and below," *IEEE Radiation Effects Data Workshop*, pp. 56-63, January 2021.

[32] A. Akkerman, J. Barak, and N.M. Yitzhak, "Role of elastic scattering of protons, muons, and electrons in inducing single event upsets," *IEEE Trans. Nucl. Sci.*, vol. 64, no. 10, pp. 2648-2660, August 2017.

[33] G. Battistoni et al., "Overview of the FLUKA code," *Ann. Nucl. Energy*, vol. 82, pp. 10-18, August 2015.

[34] T.T. Bohlen et al., "The FLUKA Code: Developments and Challenges for High Energy and Medical Applications," *Nuclear Data Sheets*, vol. 120, pp. 211-214, June 2014.